Original article

Polarity-regulated derivatization-assisted LC-MS method for amino-containing metabolites profiling in gastric cancer

Jie Han [a], Shilin Gong [a], Xiqing Bian [a], Yun Qian [b], Guilan Wang [c], Na Li [a, **], Jian-Lin Wu [a, *]

[a] *State Key Laboratory of Quality Research in Chinese Medicine, Macau Institute for Applied Research in Medicine and Health, Macau University of Science and Technology, Avenida Wai Long, Taipa, Macau, 999078, China*
[b] *Department of Gastroenterology and Hepatology, Shenzhen University General Hospital, Shenzhen, Guangdong, 518055, China*
[c] *Department of Pediatrics, Zhongshan Boai Hospital, Zhongshan, Guangdong, 528403, China*

A B S T R A C T

Amino-containing compounds, including amino acids, aliphatic amines, aromatic amines, small peptides and catecholamines, are involved in various biological processes and play vital roles in multiple metabolic pathways. Previous studies indicated that some amino-containing metabolites are significant diagnostic and prognostic biomarkers of gastric cancer. However, the discovery of precise biomarkers for the preoperative diagnosis of gastric cancer is still in an urgent need. Herein, we established a polarity-regulated derivatization method coupled with liquid chromatography-mass spectrometry (LC-MS) for amino-containing metabolites profiling in the serum samples of patients with gastric cancer and healthy controls, based on our newly designed and synthesized derivatization reagent (S)-3-(1-(diisopropoxyphosphoryl) pyrrolidine-2-carboxamido)-*N*-hydroxysuccinimidyl ester (3-DP-NHS). Enhanced separation efficiency and detection sensitivity for amino-containing metabolites were achieved after derivatization. This method exhibited good linearity, recovery, intra- and inter-day precision and accuracy. Only 5 μL serum is needed for untargeted analysis, enabling 202 amino-containing metabolites to be detected. Statistical analysis revealed altered amino acid metabolisms in patients with gastric cancer. Furthermore, ultra high performance liquid chromatography coupled with mass spectrometry (UHPLC-MS/MS) analysis quantification revealed increased serum levels of tryptamine and decreased concentrations of arginine and tryptophan in patients with gastric cancer. Receiver operating characteristic (ROC) curves indicated that an increased tryptamine/tryptophan ratio could serve as a potential biomarker for gastric cancer diagnosis. This study demostrated the possibility of using serum amino acid biomarkers for gastric cancer diagnosis, providing new avenues for the treatment of gastric cancer.

1. Introduction

Gastric cancer is the second most-common cause of cancer-related deaths worldwide. Variation in tumor biology between regions leads to differences in survival outcomes, with overall 5-year survival rates being 10%–15% in North America and 45%–50% in East Asia [1,2]. Various risk factors, such as age, sex, race, infection with *Helicobacter pylori* bacteria, and smoking are thought to be closely related to gastric cancer. In recent years, other risk factors such as pernicious anemia and a history of mucosa-associated lymphoid tissue lymphoma have been found to have

an impact on gastric cancer [3]. Gastric cancer has become a great health concern for East Asians, making early diagnosis crucial. However, as no specific symptoms are displayed in the early stages, most patients are diagnosed at an advanced stage with lymph node or remote metastasis [4]. Therefore, rapid discrimination between patients with gastric cancer and healthy people is important in the early stages of intervention.

Metabolic profiling analysis has been proven to be a practical approach for clinical diagnosis, biomarker screening, and monitoring of metabolic alteration [5,6]. It is considered as a useful tool for detecting biological alterations in biological specimens. Amino-containing compounds, including amino acids, aliphatic amines, aromatic amines, small peptides and catecholamines, etc. are involved in various important metabolic pathways. Clinical research has indicated that some of these metabolites are significant

diagnostic and prognostic biomarkers for gastric cancer [7]. Recent studies have shown that alterations in amino acid concentration may be strongly related to cancer cell proliferation and tumorigenesis [8,9]. In addition, some nervous system-associated factors, synthesized and released by both cancer cells and nerve terminals, participate in the regulation of many aspects of gastric cancer, such as cell proliferation, angiogenesis, metastasis and recurrence [10]. Hence, developing a new method for the detection and quantification of amino-containing compounds, especially amino acids and some amino-containing neurotransmitters, is essential for understanding pathological pathways, and improving the diagnosis and treatment of diseases.

Owing to its excellent performance in component separation and structure elucidation, liquid chromatography-mass spectrometry (LC-MS) is considered a suitable technology for profiling amino-containing compounds in complex matrices. Hydrophilic liquid interaction chromatography (HILIC) is a good method for analyzing highly polar compounds. However, the limitations of HILIC, such as a long re-equilibration time and less Gaussian analyte peaks [11], prompted us to turn our attention to a more robust and reproducible platform for reversed-phase chromatography. However, the relatively high polarity of most amino-containing compounds leads to weak retention and insufficient separation in commonly used reversed-phase LC (RPLC) columns. This leads to a poor response in soft ionization sources, which often results in low sensitivity, low resolution, and poor peak shape [12]. Previous reports have shown that some amino-containing metabolites, particularly neurotransmitters, are highly reactive and can be quickly oxidized or broken down once removed from the biological matrix. This inherent instability prompts the addition of stabilizing agents during derivatization processes [13]. Thus, simultaneous detection and quantification of these amino-containing compounds by RPLC remains challenging.

To solve this problem, chemical derivatization strategies have been introduced, which offer a promising approach for the sensitive detection and quantification of amino-containing compounds in RPLC-MS [14]. Generally, chemical derivatization can dramatically change the hydrophilicity of amino-containing compounds and enable good retention and separation of reversed phases [15]. Moreover, the addition of a derivatization reagent to amino groups increases the total molecular weight and eventually reduces the background noise from the matrix [16], resulting in sensitivity enhancement. N-hydroxysuccinimidyl (NHS)-containing reagents have received considerable attention because of their relatively high reactivity under mild conditions, including its carbonate, carbamate, and ester [17]. To date, multiple NHS-based derivatization reagents have been developed and applied for the analysis of amino-containing compounds. For example, 6-aminoquinolyl-N-hydroxysuccinimidyl carbamate (AQC) has been employed for the quantification of amino acids in *Arabidopsis thaliana* mutants [18]. N-hydroxysuccinimidyl carbamate (5-AIQC) was used for the measurement of amino-containing metabolites in the hemolymph of silkworms [19]. In addition, two CIL reagents, 4-dimethylaminobenzoylamido acetic acid N-hydroxylsuccinimide ester (DBAA-NHS) and 4-methoxybenzoylamido acetic acid N-hydroxylsuccinimide ester (MBAA-NHS), were used for quantitative profiling of the amine submetabolome and metabolite identification in a pooled urine sample [20]. Other NHS ester-based isobaric tag derivatization reagents, i.e., iTRAQ [21] and TMT [22], have been developed and are widely employed in proteomic workflows requiring relative quantification. NHS-based chemical derivatization with LC-MS has afforded significant improvements in amine metabolite detectability and shed light on the relationships between amino-containing metabolite biomarker discovery and the treatment of related diseases. However, some drawbacks

still exist such as relatively harsh derivatization conditions, a lack of qualitative identification of metabolites, and complex sample preparation procedures.

In this work, a novel derivatization reagent (S)-3-(1-(diisopropoxyphosphoryl) pyrrolidine-2-carboxamido)-N-hydroxysuccinimidyl ester (3-DP-NHS) was first synthesized and employed in a polarity-regulated derivatization-assisted LC-MS method for amino-containing metabolite profiling. Optimization of the derivatization conditions, chromatographic parameters, and MS parameters improved the detection sensitivity and separation efficiency of RPLC. Fragmentation analysis of the derivatized amino-containing compounds provided useful information for structural identification. Furthermore, untargeted analysis by derivatization-RPLC-high resolution mass spectrometry (HRMS) was performed using serum samples from gastric cancer patients and healthy controls. Relevant metabolic pathways and potential biomarkers in patients with gastric cancer were identified. Finally, the established method was applied to the targeted analysis of amino-containing compounds in these serum samples, and the influence of microbial metabolites on disease progression was determined.

2. Materials and methods

2.1. Chemicals and reagents

L-Methionine (Met), L-Proline (Pro), L-Phenylalanine (Phe), L-Arginine (Arg), L-Lysine (Lys), L-Cysteine (Cys), L-Asparagine (Arg) and L-Histidine (His) were supplied by Huixing Biochemical Reagent Co., Ltd (Shanghai, China). (±)-Octopamine hydrochloride (Oct), L-Tyrosine (Tyr), L-Leucine (Leu), Glycine (Gly), L-Glutamic acid (Glu), L-Valine (Val), L-Isoleucine (Ile), L-Alanine (Ala), L-Threonine (Thr), L-Tryptophan (Trp), 4-Chlorophenylalanine (4-Cl-Phe), N-hydroxysuccinimide (NHS), 1-(3-dimethylaminopropyl)-3-ethylcarbodiimide hydrochloride (EDC HCl), 1-hydroxybenzotriazole (HOBt), and ammonium acetate were purchased from Sigma-Aldrich Chemical Co. (St. Louis, MO, USA). L-Aspartic acid (Asp) and tryptamine (TRA) were purchased from J&K Chemical (Beijing, China). L-Serine (Ser) and L-Asparagine (Asn) were purchased from Macklin Biochemical Co., Ltd (Shanghai, China). 4-(2-amino-ethyl)-2-methoxy-phenol hydrochloride (3-MT), 3-(2-Methylaminoethyl) indole hydrochloride (NMTRA), 5-Hydroxytryptophan (5-HTP), serotonin (5-HT) and N-methyltyramine (NMTYA) were purchased from Toronto research chemicals (Toronto, Canada). Serotonin-α,α,β,β-d_4 (5-HT-d_4) was purchased from CDN isotopes (Quebec, Canada). Diisopropyl phosphite (DIPP) and 3-aminobenzoic acid were purchased from TCI Co., Ltd (Shanghai, China). Analytical grade triethylamine (NEt$_3$), anhydrous sodium sulfate (Na$_2$SO$_4$) and carbon tetrachloride (CCl$_4$) were obtained from Tianjin Damao Chemical Reagent Factory (Tianjin, China). LC-MS grade acetonitrile (ACN), HPLC grade methanol (MeOH), ethanol, ethyl acetate, n-hexane and dichloromethane (CH$_2$Cl$_2$) were obtained from Anaqua Chemicals Supply Inc., Ltd. (Houston, TA, USA). Ultrapure water (18.2 MΩ) was produced by a Milli-Q purification system (Millipore Corporation, Burlington, MA, USA).

2.2. Preparation of stock solutions

Stock solutions of amino-containing compounds were prepared in Milli Q water or 50% MeOH (V/V) and then serially diluted to obtain the working solutions. Three quality control (QC) working solutions at low, medium, and high concentrations were also prepared in a similar manner. In addition, 4-Cl-Phe and 5-HT-d_4 were added into the stock solution as internal standards at final

concentration of 10 ng/mL and 50 ng/mL, respectively. All standard solutions were stored at −20 °C prior to use.

2.3. Study design and patient population

Serum samples were obtained from Shenzhen University General Hospital. 10 gastric cancer patients consisting 6 males and 4 females with an average age of 64.6 ± 7.9 (mean ± standard deviation (SD)) were recruited for this study, while 15 healthy controls comprising of 8 males and 7 females with an average age of 49.3 ± 4.7 (mean ± SD) were included. All patients and healthy controls were provided informed consent for the samples and all experiments were performed in accordance with Ethics Committee Guidelines (detailed information in Table S1). Samples were stored at −80 °C before use.

2.4. Preparation of serum sample

The serum was stored at −80 °C until used. After thawing, 5 μL of serum was collected in a 1.5 mL centrifuge tube and 100 μL precool MeOH was added to precipitate the protein. After vortexed for 30 s, the mixture was centrifuged at 13,500 rpm for 5 min at 4 °C. The extraction was repeated twice and the combined supernatants were dried under a gentle nitrogen stream. The residue was stored at −20 °C before derivatization.

2.5. Synthesis of 3-DP-NHS

The derivatization reagent 3-DP-NHS was synthesized according to the described method [23–25]. In brief, 1 equiv of Pro was dissolved in triethylamine-water-ethanol (5:3:2, *V/V/V*) under stirring and the solution was cooled to 0 °C in an ice bath. A mixture of 1 equiv of DIPP in CCl_4 was added dropwise. After stirring at room temperature for 12 h, the mixture was acidified with 1 mol/L HCl to pH 2 in an ice bath and then extracted with ethyl acetate. The organic layer was collected, dried over anhydrous Na_2SO_4 and evaporated to give a yellow oily residue, which was further purified by crystallization from ethyl acetate/ n-hexane to give compound 1. 1 equiv of 3-amino benzoic acid, 2 equiv of EDC HCl, 2 equiv of *N*-hydroxysuccinimide were suspended in CH_2Cl_2 and stirred at room temperature for 4 h. After washed with water and brine, the organic layer was collected and dried over anhydrous Na_2SO_4. The solvent was removed by rotary evaporation to give compound 2 as a yellow solid. At last, 1 equiv of compound 1, 1.2 equiv of compound 2, 1.2 equiv of EDC HCl and 0.2 equiv of HOBt were mixed in CH_2Cl_2 and stirred at room temperature for 12 h. The crude product was obtained by passing the reaction mixture through a silica gel column to yield the pure white product (3-DP-NHS) (the overall yield is 19%). Both the nuclear magnetic resonance (NMR) (Figs. S1 and S2) and high-resolution mass spectrometry (Fig. S3) analysis demonstrated that 3-DP-NHS was synthesized successfully.

2.6. Chemical derivatization of amino-containing compounds by 3-DP-NHS

Ten microliters of certain concentrations of amino-containing compounds standards were added to a 1.5 mL tube, followed by 40 μL of 3 mM 3-DP-NHS and 40 μL of 10 mM NEt_3. The reaction mixture was placed in water bath at room temperature under ultrasound irradiation for 20 min (The initial water bath temperature was 18 °C and terminated at 35 °C). The reaction mixture was quenched by 10 μL of 1% formic acid solution and then dried under nitrogen stream. After drying with nitrogen gas, the residue was redissolved in 100 μL of 50% (*V/V*) ACN and 1 μL of 3-DP-NHS derivatized amine metabolites solution was subjected to LC-MS analysis.

2.7. LC-MS conditions

An Agilent 1290 Ultra-high Performance Liquid Chromatography (UHPLC) (Agilent Technologies, Santa Clara, CA, USA) consisting of an autosampler, thermostatted column compartment, and binary pump and equipped with a Waters ACQUITY UPLC®HSS T3 column (Milford, MA, USA; 2.1 × 150 mm, 1.7 μm) was applied for the separation of components. The column temperature was maintained at 40 °C. The flow rate was 0.3 mL/min without any flow splitting, and the injection volume was 1 μL. The mobile phase comprised of 10 mM ammonium acetate (A) and pure ACN (B) with the following gradient, 0–0.5 min: 20% B, 0.5–2 min: from 20% to 30.5% B, 2–5 min: 30.5% B, 5–9 min: from 30.5% to 31% B, 9–13 min: from 31% to 55% B, 13–18 min: from 55% to 85% B, 18–18.5 min: from 85% to 95% B, 18.5–21.9 min: 95% B, and 22 min: 20% B. The quantification was conducted on an Agilent 6490 iFunnel Triple Quadrupole Mass Spectrometer (QQQ-MS) with a dual Jet Stream electrospray ion source (dual AJS ESI) in positive mode. The quantification was carried out by multiple reaction monitoring (MRM) mode. Other MS parameters were set as follows: gas temperature at 225 °C, gas flow at 13 L/min, nebulizer pressure at 25 psig, sheath gas temperature at 275 °C, sheath gas flow at 12 L/min, capillary at 3,500 V, and nozzle voltage at 350 V.

For untargeted analysis, the gradient after 2 min was changed to 2–8 min: 30.5% B, 8–13 min: from 30.5% to 31% B, 13–14 min: from 31% to 55% B, 14–21 min: from 55% to 85% B, 21–23.5 min: from 85% to 95% B, 23.5–25.9 min: 95% B, and 26 min: 20% B. Untargeted profiling was conducted on an Agilent 6545 accurate-mass Q-TOF/ MS with a dual Jet stream electro-spray ion source (dual AJS ESI). The instrument was operated in positive full scan mode. The MS parameters were set as follows: gas temperature at 325 °C, dry gas flow at 11 L/min, sheath gas temperature at 350 °C, sheath gas flow at 11 L/min, nebulizer pressure at 35 psig, capillary voltage at 4,000 V, and nozzle voltage at 500 V.

2.8. Method validation

The calibration curves were constructed to quantitively measure the amino-containing metabolites. Various amounts of amino-containing compounds, ranging from 0.1 ng/mL to 1000 ng/mL, were derivatized by 3-DP-NHS, and 4-Cl-Phe and 5-HT-d_4 were utilized as internal standards (ISs). By plotting the peak area ratios (analytes/IS) versus the concentrations, the calibration curves were constructed and correlation coefficients were generated for evaluation of linearities. QC samples at low, middle, and high concentrations were analyzed 3 times in one day (intra-assay) and 3 consecutive days (inter-assay) for assessment of precision, while the accuracy was evaluated by the percentage ratio of the measured concentration to the real concentration of the QC samples. Matrix effect was performed by spiking the working solutions and internal standards into diluted serum at three concentrations and calculated by the equation of (post-extraction spiked concentration − non-spiked concentration)/spiked concentration × 100. Recovery was performed by spiking the three different concentrations of working solutions into diluted serum, and calculated by the equation of (pre-extraction spiked concentration − non-spiked concentration)/(post-extraction spiked concentration − non-spiked concentration) × 100. Stability of 3-DP-NHS derivatized amino-containing compounds was determined at 4 °C within 48 h.

2.9. Data analysis

Raw data of quantitative analysis were acquired and processed by QQQ Quantitative Analysis (Agilent Technologies). The concentrations of these analytes in samples were calculated according to the standard curves and represented as the mean ± SD. Raw data of qualitative analysis were processed with Qualitative Analysis B.06.00 software (Agilent Technology). The metabolites were automatedly classified using ClassyFire (http://classyfire.wishartlab.com/). Metabolic network pathways were constructed by Interactive Pathways Explorer (iPath) (https://pathways.embl.de/) and performed in MetaboAnalyst 3.0 (https://www.metaboanalyst.ca/). Peak areas of metabolites were acquired by MS-DIAL 4.9 with a mass tolerance of 0.01 Da automatically. Statistical significance for group discrimination was performed by *t*-test, and *P* values were adjusted using the Benjamini-Hochberg procedure, leading to the false discovery rate (FDR) adjusted *P* value. The performance of the discriminant model was characterized by estimating the area under curve (AUC) using GraphPad Prism 8.0, and the specificity, sensitivity, and accuracy were calculated.

3. Results and discussion

3.1. Derivatization reagent designing strategy

The simultaneous detection and quantification of amino-containing metabolites in biofluids are of great significance. Chemical derivatization offers an opportunity to improve the chromatographic separation and ionization efficiency of these analytes. To obtain a relatively wide detection range with high sensitivity, we aim to establish a novel derivatization method for detecting as many amino-containing metabolites as possible. First, based on previous reports, we found that an ideal derivatization reagent for amino-containing metabolite profiling should include at least the following four structural elements: (i) a structural moiety improving the ionization efficiency and hence increasing sensitivity, (ii) the ability to increase hydrophobicity to improve the retention and separation in RPLC columns, (iii) a relatively highly reactive site to facilitate chemical labeling under mild conditions, and (iv) the formation of a stable covalent linkage between the derivatization reagent and analytes through reaction, especially for highly unstable analytes (i.e., some amino-containing neurotransmitters which are prone to degradation). Our previous study demonstrated that *N*-phosphorylation labeling (DIPP) can significantly improve the detection sensitivity of AAs and peptides in electrospray ionization mass spectrometry [26]. Moreover, enhanced hydrophobicity after derivatization is crucial for improving the MS response [27]. Based on the systematic variation of these four elements and their synthetic accessibility, a novel DIPP-bearing derivatization reagent, 3-DP-NHS, was designed and synthesized using a three-step procedure (Fig. 1). In 3-DP-NHS, *N*-diisopropyl phosphite and hydrophobic moieties are expected to improve the MS response and separation efficiency, and the NHS group is expected to guarantee mild derivatization conditions. Taking these factors together, we hypothesize that this method has great potential for improving the quantification efficiency of amino-containing compounds using RPLC-MS.

To preliminarily assess the performance of 3-DP-NHS, a series of representative amino-containing metabolites, including basic, acidic, neutral, branched chain and aromatic amino acids (Arg, His, Asp, Glu, Asn, Met, Val, Phe, and Trp), as well as amino-containing neurotransmitters (3-MT and TRA), were chosen and derivatized by 3-DP-NHS, followed by ultra-high-performance liquid chromatography-quadrupole time-of-flight mass spectrometry (UHPLC-Q-TOF-MS/MS) analysis. All these compounds were
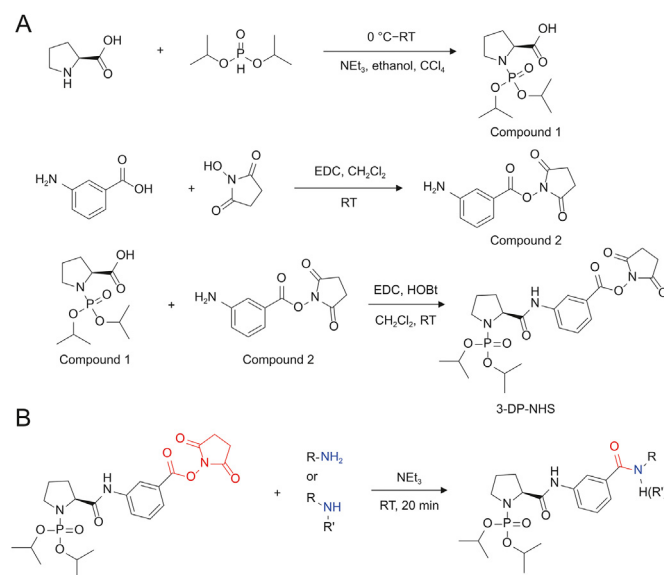

Fig. 1. (A) The synthetic route of (S)-3-(1-(diisopropoxyphosphoryl) pyrrolidine-2-carboxamido)-*N*-hydroxysuccinimidyl ester (3-DP-NHS), and (B) the chemical derivatization of amino-containing compounds by 3-DP-NHS.

successfully derivatized, and exhibited high MS responses, indicating that 3-DP-NHS is an efficient reagent for the derivatization of amino-containing metabolites (Fig. S4).

3.2. Assessment of substrate adaptability and MS characteristics

To assess the substrate scope, 20 amino acids and 7 amino-containing neurotransmitters were derivatized and analyzed. Of the 20 amino acids, 19 were successfully derivatized except for Pro. We reasoned that the steric hindrance of the cyclic amino group of Pro may hinder effective coupling with the carbonyl group of 3-DP-NHS under these reaction conditions. In addition, seven amino-containing neurotransmitters, including primary and secondary amines, were also successfully derivatized, suggesting a relatively wide substrate scope for this derivatization strategy.

The fragmentation behavior of the 3-DP-NHS derivatives was also examined, and informative fragment ions were observed. Taking valine as an example, the theoretical *m/z* values of 3-DP-NHS derivatized valine and the measured *m/z* values of the precursor and fragment ions are displayed in Fig. 2. The *m/z* value of 498.23 represented the precursor ion of 3-DP-NHS derivatized valine. The fragment ions at *m/z* 456.18 and 414.14 should be produced from the neutral loss of one or two propenes from 3-DP-NHS. The peak at *m/z* 237.12 presented a fragment ion upon cleavage of the C–N bond between the DIPP-Pro part and valine-aniline part. In addition, the other ions at *m/z* 297.06, 217.09, 234.12, 192.07, and 150.03 could be assigned to the characteristic fragments related to the derivatization reagent. In addition, *m/z* 72.08 was assigned to the iminium ion generated from Val. Furthermore, other 3-DP-NHS derivatized amino-containing compounds were examined by high-resolution mass spectrometry, and the characteristic loss of propenes and the five characteristic fragments mentioned above were observed in the MS/MS spectra of these compounds. The MS characteristics of the derivatized amino-containing compounds may further benefit the profiling of these metabolites in biological samples.

3.3. Optimization of LC-MS/MS method

A standard working solution consisting of basic, acidic, and lipophilic amino acids, as well as amino-containing
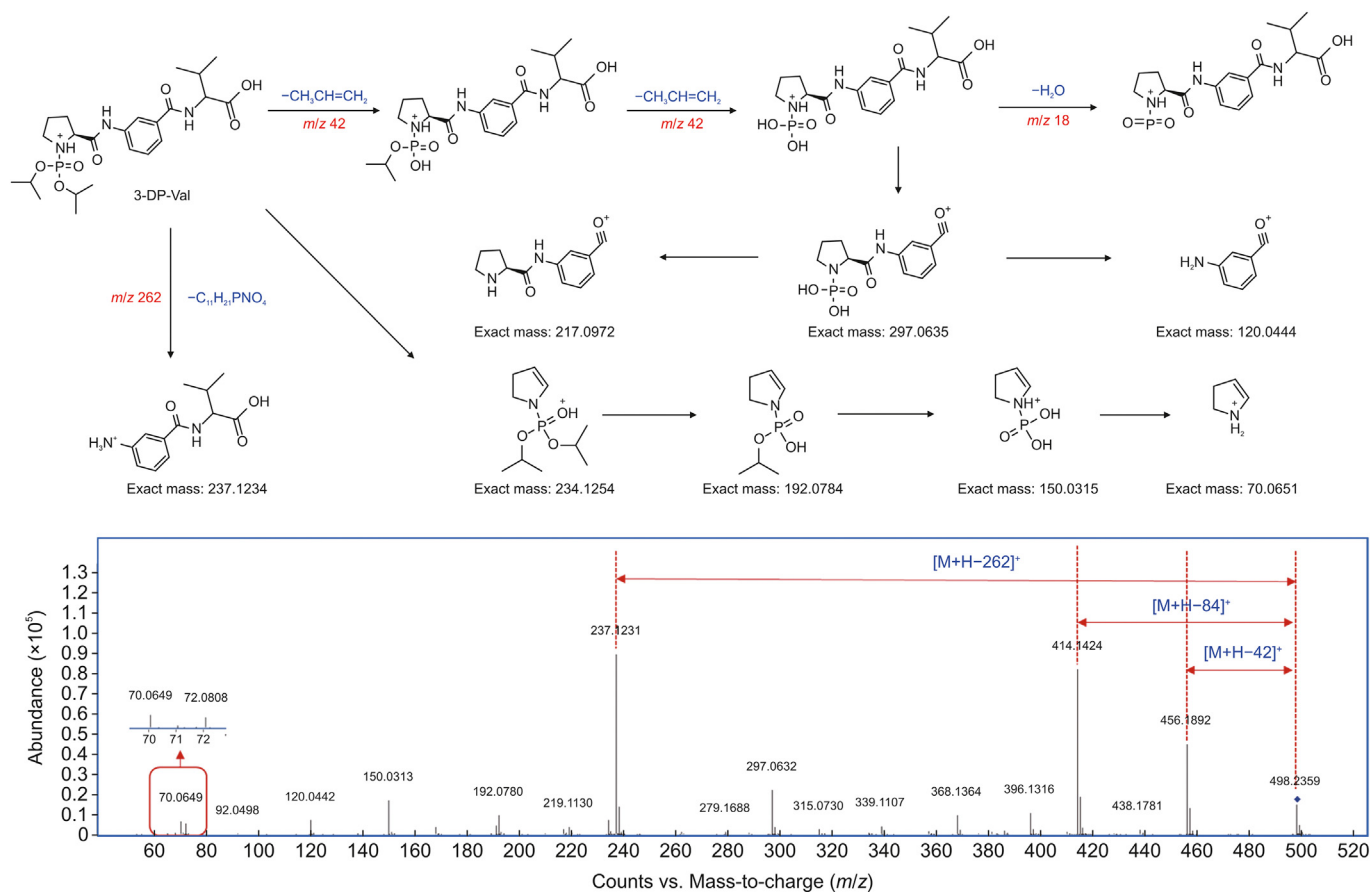
Fig. 2. MS/MS fragmentation characteristics of (S)-3-(1-(diisopropoxyphosphoryl) pyrrolidine-2-carboxamido)-*N*-hydroxysuccinimidyl ester (3-DP-NHS) derivatized valine (Val).

neurotransmitters was used to optimize the LC-MS method. First, the mobile phases of 0.1% formic acid in water and 0.1% formic acid in ACN were tested. However, the retention times of most 3-DP-NHS derivatives were markedly delayed, and a relatively long run time was required for the analysis. Subsequently, a mobile phase containing 10 mM ammonium acetate in water/pure ACN was further tested, and a relatively shorter retention time was observed. Besides, addition of 10 mM ammonium acetate to mobile phase A resulted in better MS intensities for most amino-containing compounds (Fig. S5). Therefore, 10 mM ammonium acetate was selected as the modifier. Electrospray variables, including gas temperature, gas flow, sheath gas temperature, and sheath gas flow were examined, and the results indicated that they had a slight effect on the MS intensity (Fig. S6). Furthermore, for the accurate and sensitive quantification of amino-containing metabolites in biological samples, the MRM mode was chosen, and the optimized collision energies and MRM transitions are displayed in Table S2.

3.4. Optimization of derivatization method

To obtain good labeling efficiencies using 3-DP-NHS, we optimized the labeling conditions, including reaction time, molar ratio of 3-DP-NHS, and molar ratio of NEt$_3$. Twenty-six amino-containing compounds, including 19 amino acids and 7 amino-containing neurotransmitters were selected as analytes for reaction optimization. Different ultrasonication times were tested, and the results showed that the peak areas of the derivatives increased with time from 5 to 20 min and gradually plateaued at 30 min (Fig. 3A).

Therefore, a reaction time of 20 min was selected. The concentration of 3-DP-NHS was optimized to range from 0.5 mM to 5 mM. The results showed that the peak areas of the products plateaued when the concentration of 3-DP-NHS was 3 mM (Fig. 3B). Next, the concentration of the base was optimized using 3 mM 3-DP-NHS. The peak areas of the derivatives were in a relatively low level in the presence of 1 mM NEt$_3$, indicating that an alkaline environment is essential for the initiation of derivatization. We reasoned that the elimination of NHS could proceed smoothly because of the relatively stronger nucleophilicity of the deprotonated amine under alkaline conditions [28]. Upon increasing the concentration of NEt$_3$ to 5 mM, the peak areas increased sharply, eventually plateauing at 10 mM (Fig. 3C). Taken together, the optimal conditions for the chemical labeling reaction were determined to be in a water bath for 20 min of ultrasonication, and the concentrations of 3-DP-NHS and NEt$_3$ were 3 mM and 10 mM, respectively.

3.5. Analytical performance of 3-DP-NHS derivatization

Next, the performance of the proposed method was evaluated. By introducing a relatively strong hydrophobic group to the amino group, the retention times of hydrophilic amino containing compounds, including 19 amino acids and 7 amino-containing neurotransmitters, were greatly prolonged. Before derivatization, all of the analytes were flushed out between 1.18 and 3.41 min with distorted peak shapes, leading to more co-elution compounds and severe peaks overlapping. However, after derivatization by 3-DP-NHS, the retention times were delayed to 3.03–15.55 min, and significant improvements in peak shapes were observed (Fig. 4).
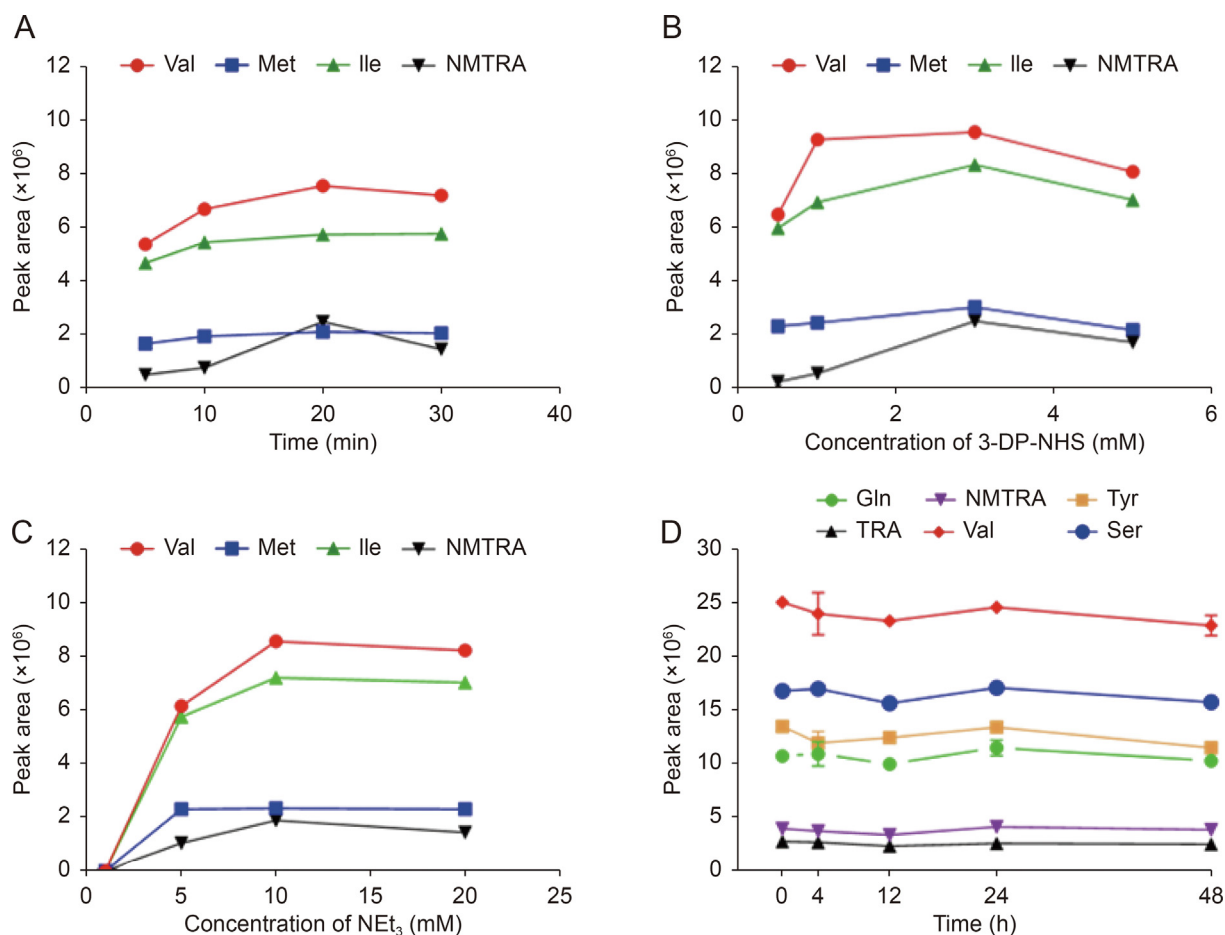
Fig. 3. (A) Optimization of reaction time. (B) Optimization of concentration of (S)-3-(1-(diisopropoxyphosphoryl) pyrrolidine-2-carboxamido)-N-hydroxysuccinimidyl ester (3-DP-NHS). (C) Optimization of concentration of NEt₃. (D) Validation of the stability of 3-DP-NHS derivative products. NEt₃: triethylamine; Val: valine; Met: methionine; Ile: isoleucine; NMTRA: 3-(2-methylaminoethyl) indole; Tyr: tyrosine; TRA: tryptamine; Ser: serine.

As a result, the improved separation efficiency allowed for good separation of difficult-to-discriminate isomeric amino-containing compounds. For example, a pair of isomeric compounds, that is, Leu (peak 17) and Ile (peak 16), could be baseline separated by RPLC after 3-DP-NHS derivatization although they share the same precursor ion, product ion and collision energy. In addition, some amino-containing neurotransmitters with similar chemical features could be distinguished after derivatization. For instance, TRA (peak 25), NMTRA (peak 26), 5-HT (peak 22), and 5-HTP (peak 14) are indole analogs with slight structural differences in their functional groups. After 3-DP-NHS derivatization, their separation efficiency of the RPLC column improved, further facilitating the discrimination of these low-concentration metabolites from the complex matrix.

Moreover, the limit of detection (LOD) of the 3-DP-NHS derivatization was calculated and compared with that of a previously reported DIPP derivatization method (Table S3). Using Tyr as an example, the LOD of the 3-DP-NHS derivative was 350-fold lower than that of the DIPP derivative. Other 3-DP-NHS derivatized AAs also showed lower LODs than the DIPP derivatives except for Gly, Asp, and Asn. We speculated that the more hydrophobic characteristics of the 3-DP-NHS derivatives were responsible for the surface activity enhancement, which improved ion emission from the charged droplets formed in the ESI, resulting in improved ionization efficiency [29]. Another advantage of our method is that no additional sample pretreatment is required prior to LC-MS/MS

analysis. In contrast, a desalination procedure by C18 solid-phase extraction column must be conducted to remove the organic salts during DIPP derivatization prior to LC-MS/MS analysis [30], which further extends the total analysis time. These results proved that this derivatization greatly enhanced the separation ability and detection sensitivity and enabled the simultaneous detection of polar amino-containing compounds.

3.6. Method validation

The LC-QQQ-MS method was validated for LOD, limit of quantification (LOQ), linearity, reproducibility, accuracy, recovery, and matrix effects. Good linearities of the target analytes were exhibited, with satisfactory correlation coefficients (R^2) greater than 0.99 (except for Oct and Cys) (Table S3). The LODs and LOQs of amino-containing compounds were in the range of 0.03–8.3 ng/mL and 0.1–25 ng/mL, respectively. The intra-day and inter-day relative standard deviations (RSDs) were below 17.86%, and the accuracies were in the range of 79.33%–116.04% (Table S4). The recoveries were 72.3%–118.4% for low, medium, and high levels of spiked serum samples. The matrix effect values were in the range of 76.3%–121.3% (Table S5). These results showed that our method could determine amino-containing compounds sensitively and accurately, which also indicated a high labeling efficiency. Moreover, 3-DP-NHS derivatives were stable for at least 48 h (Fig. 3D). Increased stability is crucial for some biogenetic amines, especially
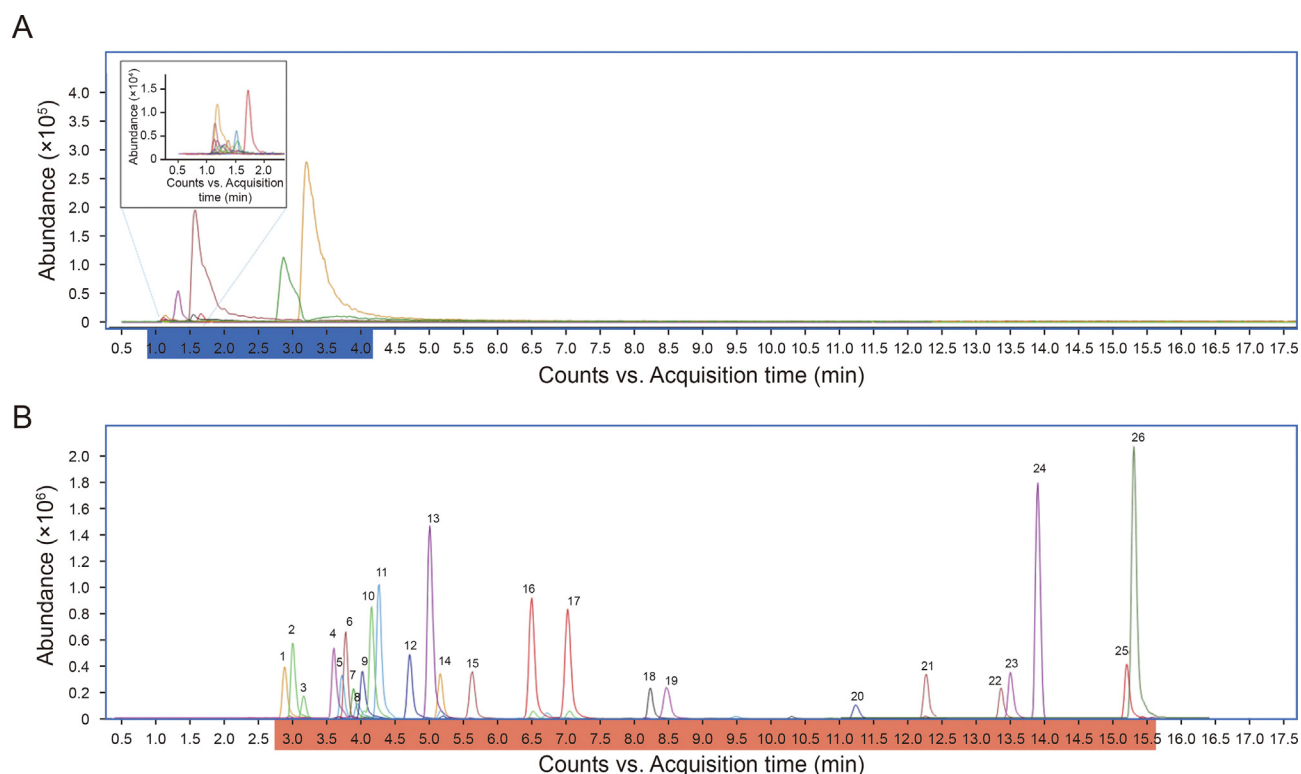
A

B

Fig. 4. Multiple reaction monitoring (MRM) chromatograms of amino-containing metabolites. (A) MRM chromatograms of non-derivatized amino-containing metabolites. (B) MRM chromatograms of (S)-3-(1-(diisopropoxyphosphoryl) pyrrolidine-2-carboxamido)-N-hydroxysuccinimidyl ester (3-DP-NHS) derivatized amino-containing metabolites. (1) Asp; (2) Glu; (3) Asn; (4) Ser; (5) Gln; (6) His; (7) Gly; (8) Cys; (9) Thr; (10) Ala; (11) Arg; (12) Tyr; (13) Val; (14) 5-HTP; (15) Met; (16) Ile; (17) Leu; (18) Phe; (19) Trp; (20) Oct; (21) Lys; (22) 5-HT; (23) 3-MT; (24) NMTYA; (25) TRA; (26) NMTRA. Asp: aspartic acid; Glu: glutamic acid; Asn: asparagine; Ser: serine; Gln: glutamine; His: histidine; Gly: glycine; Cys: cysteine; Thr: threonine; Ala: alanine; Arg: arginine; Tyr: tyrosine; Val: valine; 5-HTP: 5-hydroxytryptophan; Met: methionine; Ile: isoleucine; Leu: leucine; Phe: phenylalanine; Trp: tryptophan; Oct: octopamine; Lys: lysine; 5-HT: serotonin; 3-MT: 4-(2-amino-ethyl)-2-methoxy-phenol; NMTYA: N-methyltyramine; TRA: tryptamine; NMTRA: 3-(2-methylaminoethyl) indole.

catecholamines, which are prone to rapid degradation through auto-oxidation via the radical pathway [13]. Thus, this method can provide reproducible quantification of amino-containing compounds in complex matrices.

Compared to previous methods, our method showed a significant improvement in sensitivity (relatively lower LOQs) with a smaller sample volume (as low as 5 μL) (Table S6). This is beneficial for clinical diagnosis because less blood is required from the patients. In addition, the derivatization occurring at room temperature in this approach is quicker and milder than methods with heating (Table S6), which enables the detection of thermally sensitive and unstable compounds.

3.7. Untargeted analysis of amino-containing metabolites in patients with gastric cancer

As mentioned in the introduction, amino-containing metabolites are involved in many metabolic pathways, some of which may be related to the diagnosis and prognosis of gastric cancer. Therefore, we attempted to detect and identify as many unknown amino-containing metabolites as possible in patients with gastric cancer using our developed approach to understand the correlation between these metabolites and gastric cancer.

The derivatized amino-containing metabolites were identified based on their MS and MS/MS fragmentation characteristics as follows: First, the m/z of the molecular ion of the original amino-containing metabolites was calculated from the determined m/z by subtracting 380.1496, derived from the addition of $C_{18}H_{25}N_2O_5P$ by 3-DP-NHS derivatization. The obtained m/z values

were then searched against online metabolomics databases, such as HMDB [31] and METLIN [32]. Amino-containing metabolites were identified by restricting the tolerance range of the query m/z value and analyzing the MS/MS fragmentation pattern. Consequently, 202 amino-containing metabolites with molecular weights ranging from 17 to 317 were selected, covering a wide molecular range of amine metabolites. The results showed that 3-DP-NHS derivatization has another advantage: it can be applied to the identification of low-molecular-weight metabolites. For example, metabolite with m/z 18.0344 was identified as ammonia, which has been proven to be associated with the progression of fibrosis in non-alcoholic fatty liver disease and hepatic encephalopathy severity [33,34]. Moreover, derivatization prevented interference from the low m/z region with small-molecule amino-containing compounds.

To accurately and quickly elucidate the metabolic fate of these metabolites in patients with gastric cancer, ClassyFire was employed to automatically assign these metabolites into 7 superclasses, 18 classes, and 23 subclasses (Fig. 5). At superclass levels, these metabolites were mostly assigned as "Organic acids and derivatives" and "Organic nitrogen compounds." Among the class levels, "Carboxylic acids and derivatives" were the main classes. Moreover, "Amino acids, peptides and analogs" and "Amines" were the main two subclasses.

The levels of these metabolites were compared using fold changes between patients with gastric cancer and healthy controls. Among these identified metabolites, 17 were significantly enriched, whereas 54 were significantly depleted in the gastric cancer patient group (FDR adjusted P < 0.05). In addition, iPath was used to
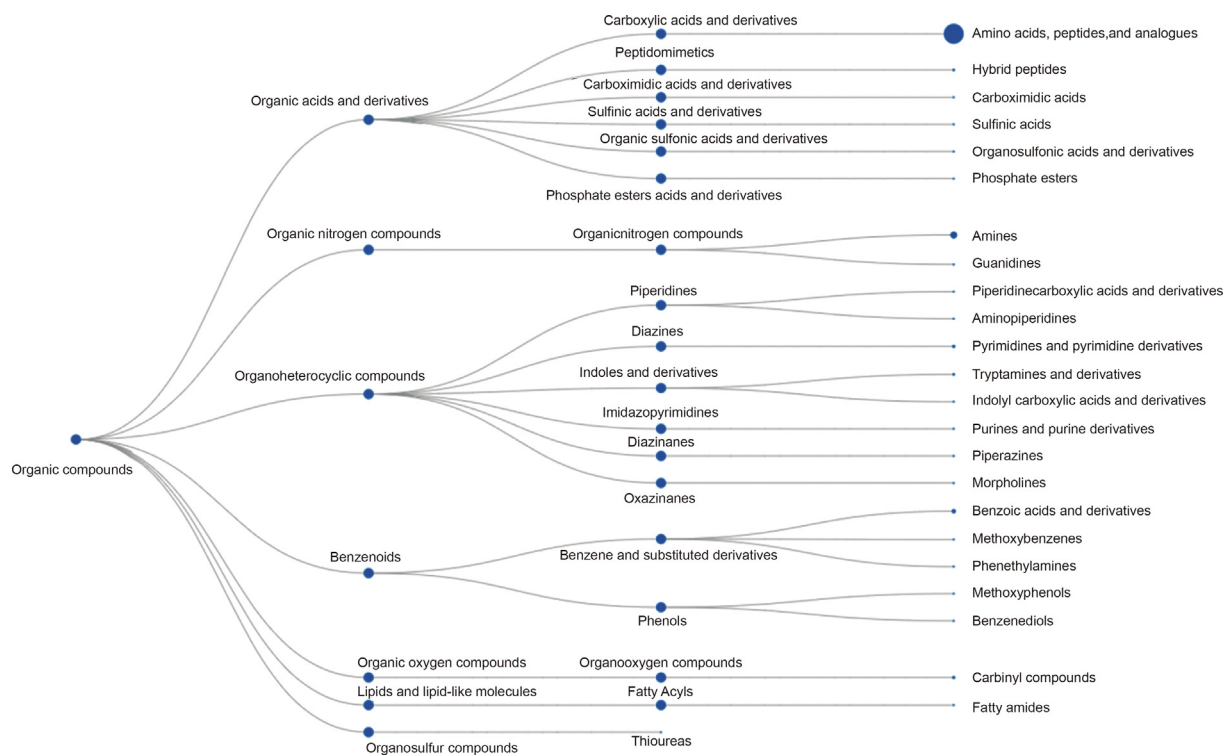
Fig. 5. Metabolomic pipeline using ClassyFire.
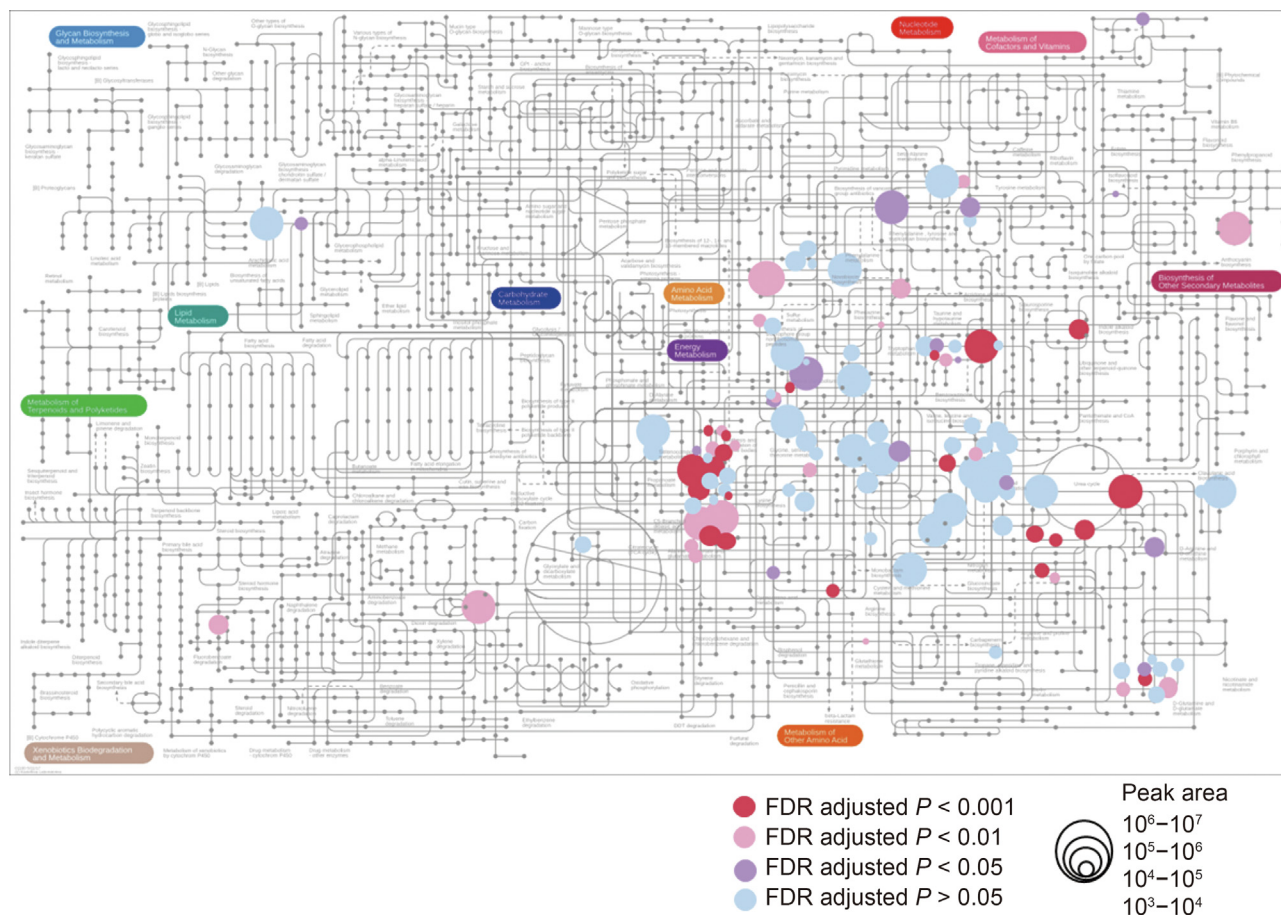
Fig. 6. IPath analysis. iPath 3.0 is a tool (https://pathways.embl.de/) for metabolic network pathways. FDR: false discovery rate.

construct metabolic pathways based on Kyoto Encyclopedia of Genes and Genomes (KEGG) annotations. Differential metabolic pathways in patient with gastric cancer, especially amino acids, peptides and analogs, were quickly identified (Fig. 6). Pathway enrichment analysis was conducted using MetaboAnalyst, and the results indicated that glycine and serine metabolism, urea cycle, Trp metabolism, and taurine and hypotaurine metabolism were the main differential metabolic pathways (Fig. 7A). Ornithine, Arg, 3-methyl-histidine, L-carnosine, 5-aminolevlinic acid, hypotaurine, Trp, and TRA were identified as relevant metabolites (Fig. 7B). The receiver operating characteristic (ROC) curves of these metabolites were created to demonstrate their predictive power, and the AUC values were calculated (Fig. 7C, and Table 1). These results indicated that Arg, Trp and TRA, which have higher AUC values than the others, could discriminate patients with gastric cancer from healthy humans and might be potential biomarkers.

3.8. Validation of differential metabolites for potential biomarker discovery

Previous studies, as along with our untargeted analysis, have shown that amino acid metabolism is notably altered in cancer cells and patients. Moreover, accurate quantification of specific metabolites in complex biological samples using targeted metabolomics can shed light on potential biomarker discovery and accurate biological interpretation of metabolites in gastric cancer. For a deeper understanding of the metabolic alterations in gastric cancer, the developed MRM method was applied for the quantification of targeted amino-containing compounds in the serum of patients with gastric cancer and healthy controls (Table 2). The results suggested that 19 natural amino acids and 4 amino-containing neurotransmitters were successfully detected in serum samples with concentrations ranging from 0.41 ng/mL to 139.47 μg/mL. However, some trace amines such as Oct, 3-MT, and 5-HTP could not be quantified as their concentrations were below the LOQs.

Subsequent statistical analyses were performed to identify the variations in these metabolites among the different groups (FDR adjusted $P < 0.05$). According to the t-test results, three metabolites were identified as significant differential metabolites in patients with gastric cancer compared to those in healthy controls. The levels of Trp (FDR adjusted $P = 0.004$) and Arg (FDR adjusted $P = 0.046$) were significantly decreased in the serum of patients with gastric cancer compared to those in healthy controls, while serum levels of TRA (FDR adjusted $P = 0.039$) were increased, which is consistent with our untargeted analysis results (Fig. 8A). Average concentrations of Trp, Arg, and TRA were 17.03 μg/mL, 22.50 μg/mL, 0.097 μg/mL and 11.57 μg/mL, 14.39 μg/mL, 0.12 μg/mL, respectively, in serum samples of healthy control and gastric cancer groups. In addition, a significantly higher TRA/Trp ratio (FDR adjusted $P = 0.0041$) was observed in the gastric cancer group.

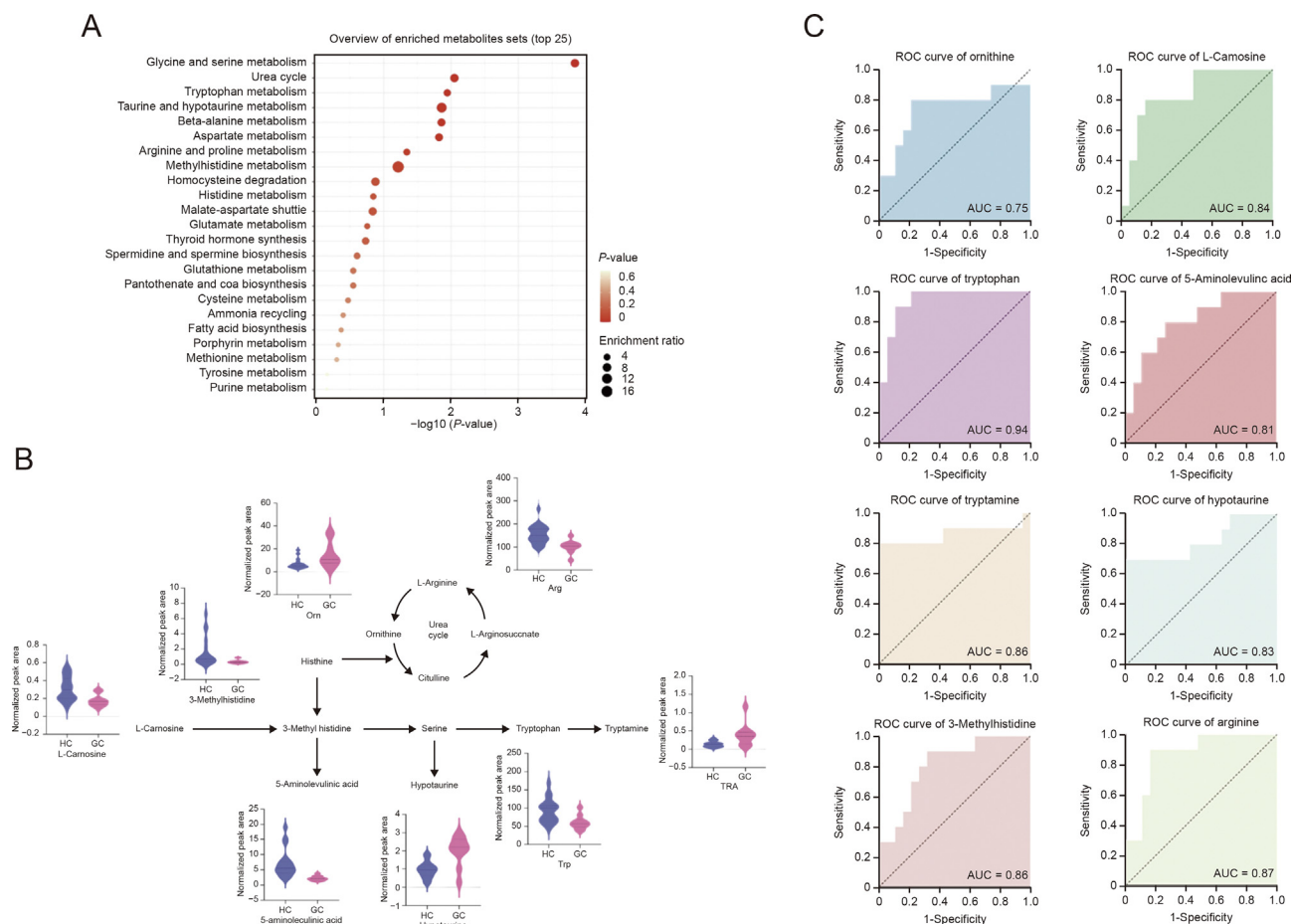
Fig. 7. (A) Pathway enrichment analysis of differential metabolites. (B) Changes of the relevant metabolites between gastric cancer patients and healthy controls. (C) Receiver operating characteristic (ROC) curves of differential metabolites.

Table 1
The area under curve (AUC) values, 95% confidence interval (95%CI), sensitivity, specificity, accuracy, false discovery rate (FDR) adjusted P value and fold change of significantly changed metabolites between gastric cancer patients and healthy controls.

Name	AUC	95%CI	Sensitivity (%)	Specificity (%)	Accuracy (%)	FDR adjusted P value	Fold change[a]
Ornithine	0.75	0.53–0.97	80	79.0	79.5	0.039	1.75
Carnosine	0.84	0.69–0.99	80	84.2	82.1	0.0062	−2.01
Tryptophan	0.94	0.86–1.00	90	89.5	89.8	0.00013	−1.83
5-aminolevulinic acid	0.81	0.65–0.97	80	73.7	76.9	0.0044	−3.70
Tryptamine	0.86	0.67–1.00	80	94.7	87.4	0.0082	1.97
Hypotaurine	0.83	0.64–1.00	70	100.0	85.0	0.0087	1.86
3-methylhistidine	0.81	0.65–0.97	90	68.4	79.2	0.026	−2.20
Arginine	0.87	0.74–1.00	90	84.2	87.1	0.0051	−1.77

[a] Fold change was calculated by comparing gastric cancer patient group with healthy controls. Fold change value with a positive value indicates a relatively higher concentration present in gastric cancer group, while a negative value means a relative lower concentration as compared to the control group.

The diagnostic value of potential gastric cancer biomarkers was evaluated using ROC curves. The AUC values, sensitivity, specificity, and accuracy of Arg, TRA, Trp, and the TRA/Trp ratio were calculated. Compared to the untargeted analysis results, the AUC values of Arg and TRA were slightly lower, whereas the AUC value of Trp was comparable. From the perspective of quantitative accuracy, we believe that absolute quantification results can reflect the state of organisms more accurately. Among these four items, the TRA/Trp ratio exhibited a higher AUC value, along with acceptable sensitivity, specificity, and accuracy (sensitivity, 91.4%; specificity, 87.5%; 95% confidence interval (95%CI), 0.8085–0.9391) (Fig. 8B). In this case, we deduced that the TRA/Trp ratio is a suitable biomarker for the diagnosis of gastric cancer.

3.9. Biological interpretation of potential biomarkers

The Warburg effect in tumor cells involves enhanced glycolysis to generate energy under aerobic conditions. Abnormal glucose metabolism in cancer cells is associated with amino acid metabolism. Altered amino acid concentrations in patients with gastric

Table 2
Absolute quantification of amino-containing metabolites in serum of healthy controls (HC) and gastric cancer (GC) patients[a].

No.	Name	HC (μg/mL)	GC patients (μg/mL)
1	Gln	67.71 ± 19.96	65.13 ± 27.03
2	Glu	67.99 ± 32.11	78.18 ± 37.11
3	His	24.52 ± 5.48	24.95 ± 14.10
4	Thr	40.92 ± 7.17	39.17 ± 19.98
5	Ala	34.36 ± 5.71	35.08 ± 12.20
6	Arg	22.50 ± 6.51	14.39 ± 8.44
7	Tyr	9.18 ± 2.73	7.76 ± 2.44
8	Val	28.13 ± 6.26	30.15 ± 13.34
9	Trp	17.03 ± 2.40	11.57 ± 3.04
10	Ile	10.89 ± 2.57	12.44 ± 6.68
11	Leu	19.29 ± 4.72	18.78 ± 6.56
12	Phe	18.86 ± 4.04	24.37 ± 12.95
13	Asp	8.52 ± 2.95	9.22 ± 7.76
14	Asn	5.07 ± 1.06	4.69 ± 2.24
15	Ser	32.15 ± 4.73	35.68 ± 17.64
16	Gly	139.47 ± 16.83	124.99 ± 49.29
17	Met	3.86 ± 0.74	5.58 ± 5.26
18	Lys	16.66 ± 5.53	14.03 ± 6.62
19	Cys	6.33 ± 0.45	5.79 ± 0.51
20	NMTYA	0.00044 ± 0.000079	0.00041 ± 0.000042
21	TRA	0.097 ± 0.01	0.12 ± 0.031
22	NMTRA	0.00041 ± 0.00023	0.00056 ± 0.00053
23	5-HT	0.62 ± 0.04	0.44 ± 0.05

[a] Data were shown as average ± standard deviation.
Gln: glutamine; Glu: glutamic acid; His: histidine; Thr: threonine; Ala: alanine; Arg: arginine; Tyr: tyrosine; Val: valine; Trp: tryptophan; Ile: isoleucine; Leu: leucine; Phe: phenylalanine; Asp: aspartic acid; Asn: asparagine; Ser: serine; Gly: glycine; Met: methionine; Lys: lysine; Cys: cysteine; NMTYA: N-methyltyramine; TRA: tryptamine; NMTRA: 3-(2-methylaminoethyl) indole; 5-HT: serotonin.
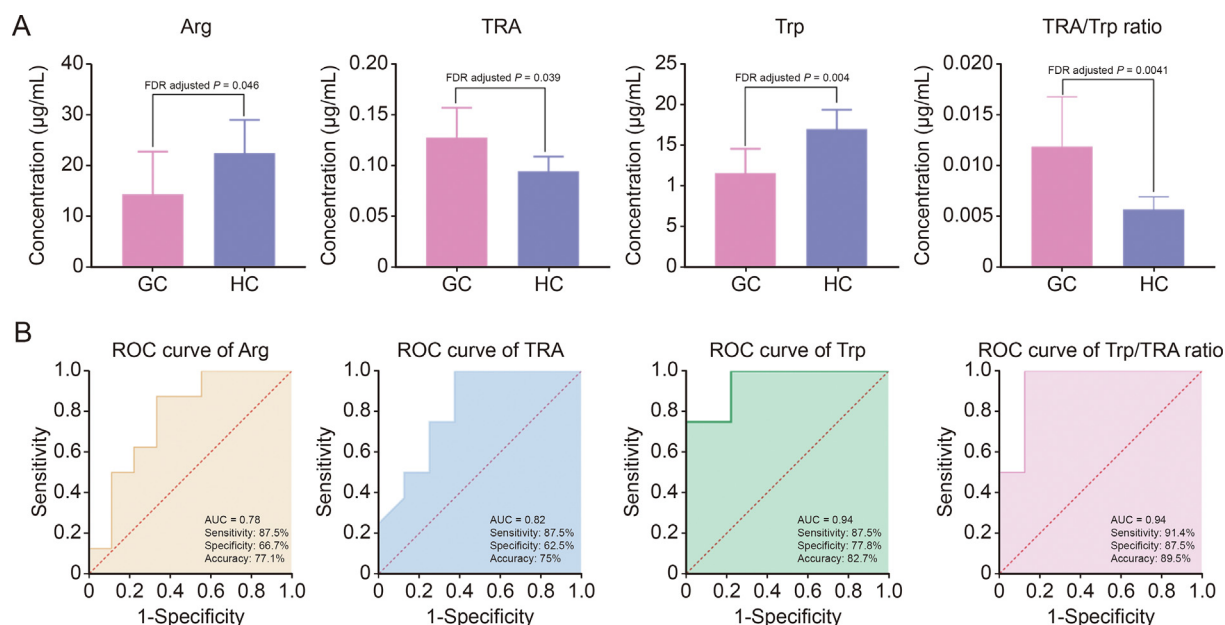
cancer indicate an imbalance in amino acid or energy metabolism in gastric cancer.

In our study, Trp was downregulated in the serum of patients with gastric cancer, while its downstream metabolites were upregulated, including TRA and kynurenine (with no statistical significance). These results suggested that altered Trp metabolism is closely associated with the development of gastric cancer. Trp is thought to exert complex multifaceted biological effects. It was reported that over 95% of the absorbed Trp is catalyzed via the kynurenine pathway, which was strongly bound to gastric cancer cells, while only 1%–2% and 2%–3% of dietary Trp is converted into serotonin and indole pathways, respectively [35,36]. The decrease in Trp observed in our study may have been induced by the activation of the Trp-metabolizing enzymes indoleamine 2,3-dioxygenase (IDO) and tryptophan dioxygenase (TDO), which are frequently activated in cancer, leading to the consumption of Trp in cancers [37–42]. These studies may explain the downregulation of Trp observed in our study.

TRA, a downstream metabolite of Trp metabolism in the indole pathway was upregulated in the serum of the patients in our research. It was reported that TRA is a β-arylamine neurotransmitter that can potentiate the inhibitory response of cells to serotonin [43]. The increase in TRA levels may be induced by Trp decarboxylase, which converts Trp to TRA and is produced by *Clostridium sporogenes* [44,45]. This gram-positive *Bacillus* strain was found to be increased in the gut microbiota of patients with gastric cancer, and eventually led to an enhanced release of transcription factors, oncogenes, and inflammation genes by producing toxic factor adhesion A on the cell surface. *Clostridium sporogenes* was also found to colonize in the gastric microenvironment of patients with gastric cancer [46,47]. Therefore, the observed enhancement of TRA may be induced by the increase in *Clostridium sporogenes* in the gut microbiota of patients with gastric cancer, which accounted for increased Trp decarboxylase activity and improved the conversion from Trp to TRA.

Downregulation of arginases in patient with gastric cancer was also observed in our study. Early studies reported elevated arginase levels in gastric cancer cell lines, serum, and tissues from patients with gastric cancer [48,49]. Recently, it has been shown that arginase I production in the tumor microenvironment by mature myeloid cells is responsible for reduced levels of Arg, revealing that arginase is closely related to curbing the response of antitumor T lymphocytes in gastric cancer [50,51]. Increased expression of arginase I consumes more Arg, leading to decreased levels of Arg for accelerated growth of tumor cells in the tumor microenvironment. This finding is consistent with our results.

According to our results, the variation in Trp, TRA, and Arg levels in gastric cancer patients might be involved in the kynurenine and indole pathways, as well as influenced by *Clostridium sporogenes* levels and arginase abundance. However, confounding factors such as age, sex, and lifestyle may also affect the serum levels of amino

Fig. 8. (A) Comparison of absolute concentration of Arg, TRA, Trp, and TRA/Trp ratio between gastric cancer (GC) patients and healthy controls (HC). (B) Receiver operating characteristic (ROC) curve of differential metabolites based on absolute quantification. Arg: arginine; TRA: tryptamine; Trp: tryptophan.

acids and other amino-containing metabolites. The sample size used in the study was not large enough to generate an efficient discussion about potential influence, which awaits a more comprehensive investigation using a larger cohort of patients and healthy controls.

4. Conclusions

In this study, a polarity-regulated 3-DP-NHS derivatization method coupled with UHPLC-Q-TOF/MS and UHPLC-MS/MS analyse was introduced to profile of amino-containing metabolites. A novel *N*-hydroxysuccinimide-based derivatization reagent, 3-DP-NHS, was designed and synthesized using a three-step procedure, that significantly enhanced the ionization efficiency and increased the separation performance of amino-containing compounds in RPLC-MS. In addition, various amino-containing compounds, including primary and secondary amines, can be derivatized by 3-DP-NHS. The developed method enabled the untargeted profiling of 202 amino-containing metabolites in 5 μL serum samples from gastric cancer patients and healthy controls, in which 71 differential metabolites and the main differential metabolic pathways were revealed. Quantitative analysis of differential amino-containing metabolites further indicated a significant correlation between the TRA/Trp ratio and gastric cancer, which could be used for diagnosis with a predictive accuracy of 89.5%. Moreover, the potential of the TRA/Trp ratio as a biomarker for gastric cancer may inspire the early diagnosis of gastric cancer as well as benefit treatment response monitoring and prognosis prediction in patients with gastric cancer. In addition, this study provides new insights and methods for patient-centric sampling-assisted personalized healthcare. Further investigations based on a larger cohort of patients with gastric cancer and healthy controls will be conducted to understand the biological relevance of the TRA/Trp ratio and the underlying mechanisms of its association with gastric cancer.

CRediT author statement

Jie Han: Methodology, Data curation, Investigation, Writing - Original draft preparation; **Shilin Gong:** Methodology, Writing - Original draft preparation; **Xiqing Bian:** Methodology,

Investigation; **Yun Qian:** Resources, Formal analysis; **Guilan Wang:** Formal analysis; **Na Li:** Conceptualization, Supervision, Writing - Reviewing and Editing; **Jian-Lin Wu:** Conceptualization, Supervision, Writing - Reviewing and Editing.

Declaration of competing interest

The authors declare that there are no conflicts of interest.

Acknowledgments

Appendix A. Supplementary data

Supplementary data to this article can be found online at https://doi.org/10.1016/j.jpha.2023.06.009.

References

[1] W.J. Lee, W.C. Lee, S.J. Houng, et al., Survival after resection of gastric cancer and prognostic relevance of systematic lymph node dissection: Twenty years experience in Taiwan, World J. Surg. 19 (1995) 707–713.
[2] Y.J. Mok, B.W. Koo, C.W. Whang, et al., Cancer of the stomach: A review of two hospitals in Korea and Japan, World J. Surg. 17 (1993) 777–782.
[3] S.S. Joshi, B.D. Badgwell, Current treatment and recent progress in gastric cancer, CA Cancer, J. Clin. 71 (2021) 264–279.
[4] Y. Chen, J. Zhang, L. Guo, et al., A characteristic biosignature for discrimination of gastric cancer from healthy population by high throughput GC-MS analysis, Oncotarget 7 (2016) 87496–87510.
[5] X. Song, X. Yang, R. Narayanan, et al., Oral squamous cell carcinoma diagnosed from saliva metabolic profiling, Proc. Natl. Acad. Sci. U. S. A. 117 (2020) 16167–16173.
[6] E.C. Chan, K.K. Pasikanti, J.K. Nicholson, Global urinary metabolic profiling procedures using gas chromatography-mass spectrometry, Nat. Protoc. 6 (2011) 1483–1499.
[7] R. Maejima, K. Tamai, T. Shiroki, et al., Enhanced expression of semaphorin 3E is involved in the gastric cancer development, Int. J. Oncol. 49 (2016) 887–894.

[8] M. Jain, R. Nilsson, S. Sharma, et al., Metabolite profiling identifies a key role for *Glycine* in rapid cancer cell proliferation, Science 336 (2012) 1040–1044.

[9] W. Zhang, N. Shyh-Chang, H. Yang, et al., *Glycine* decarboxylase activity drives non-small cell lung cancer tumor-initiating cells and tumorigenesis, Cell 148 (2012) 259–272.

[10] K. Wang, X. Zhao, J. Liu, et al., Nervous system and gastric cancer, Biochim. Biophys. Acta Rev. Cancer 1873 (2020), 188313.

[11] V. Sagi-Kiss, Y. Li, M.R. Carey, et al., Ion-pairing chromatography and amine derivatization provide complementary approaches for the targeted LC-MS analysis of the polar metabolome, J. Proteome Res. 21 (2022) 1428–1437.

[12] E. Öztürk Er, S. Erarpat, S. Bodur, et al., Accurate determination of amino acids by quadruple isotope dilution-reverse phase liquid Chromatography-Tandem mass spectrometry after derivatization with 2-Naphthoyl chloride, J. Chromatogr. A 1667 (2022), 462870.

[13] B.A. Boughton, D.L. Callahan, C. Silva, et al., Comprehensive profiling and quantitation of amine group containing metabolites, Anal. Chem. 83 (2011) 7523–7530.

[14] X. Bian, Y. Zhang, N. Li, et al., Ultrasensitive quantification of trace amines based on *N*-phosphorylation labeling chip 2D LC-QQQ/MS, J. Pharm. Anal. 13 (2023) 315–322.

[15] X. Bian, N. Li, B. Tan, et al., Polarity-tuning derivatization-LC-MS approach for probing global carboxyl-containing metabolites in colorectal cancer, Anal. Chem. 90 (2018) 11210–11215.

[16] T. Santa, Derivatization reagents in liquid chromatography/electrospray ionization tandem mass spectrometry, Biomed. Chromatogr. 25 (2011) 1–10.

[17] C. Papamicaël, V. Gembus, A. Barré, et al., An overview of the synthesis of highly versatile N-hydroxysuccinimide esters, Synthesis 49 (2016) 472–483.

[18] C. Salazar, J.M. Armenta, V. Shulaev, An UPLC-ESI-MS/MS assay using 6-aminoquinolyl-N-hydroxysuccinimidyl carbamate derivatization for targeted amino acid analysis: Application to screening of *Arabidopsis thaliana* mutants, Metabolites 2 (2012) 398–428.

[19] J. Wang, L. Zhou, H. Lei, et al., Simultaneous quantification of amino metabolites in multiple metabolic pathways using ultra-high performance liquid chromatography with tandem-mass spectrometry, Sci. Rep. 7 (2017), 1423.

[20] R. Zhou, T. Huan, L. Li, Development of versatile isotopic labeling reagents for profiling the amine submetabolome by liquid chromatography-mass spectrometry, Anal. Chim. Acta 881 (2015) 107–116.

[21] C. Evans, J. Noirel, S.Y. Ow, et al., An insight into iTRAQ: Where do we stand now? Anal. Bioanal. Chem. 404 (2012) 1011–1027.

[22] J.P. Murphy, R.A. Everley, J.L. Coloff, et al., Combining amine metabolomics and quantitative proteomics of cancer cells using derivatization with isobaric tags, Anal. Chem. 86 (2014) 3585–3593.

[23] K. Shen, L. Wang, Q. He, et al., Sensitive bromine-labeled probe D-BPBr for simultaneous identification and quantification of chiral amino acids and amino-containing metabolites profiling in human biofluid by HPLC/MS, Anal. Chem. 92 (2020) 1763–1769.

[24] G.J. Ji, C.B. Xue, J.N. Zeng, et al., Synthesis of *N*-(Diisopropyloxyphosphoryl) amino acids and peptides, Synthesis-Stuttgart 6 (1988) 444–448.

[25] D.W. Domaille, J.N. Cha, Aniline-terminated DNA catalyzes rapid DNA-hydrazone formation at physiological pH, Chem. Commun. 50 (2014) 3831–3833.

[26] X. Hu, X. Bian, W. Gu, et al., Stand out from matrix: Ultra-sensitive LC-MS/MS method for determination of histamine in complex biological samples using derivatization and solid phase extraction, Talanta 225 (2021), 122056.

[27] J. Leng, H. Wang, L. Zhang, et al., A highly sensitive isotope-coded derivatization method and its application for the mass spectrometric analysis of analytes containing the carboxyl group, Anal. Chim. Acta 758 (2013) 114–121.

[28] S. Mädler, C. Bich, D. Touboul, et al., Chemical cross-linking with NHS esters: A systematic study on amino acid reactivities, J. Mass Spectrom. 44 (2009) 694–706.

[29] S. Zhao, L. Li, Chemical derivatization in LC-MS-based metabolomics study, Trac Trends Anal. Chem. 131 (2020), 115988.

[30] X. Chen, D. Gao, F. Liu, et al., A novel quantification method for analysis of twenty natural amino acids in human serum based on N-phosphorylation labeling using reversed-phase liquid chromatography-tandem mass spectrometry, Anal. Chim. Acta 836 (2014) 61–71.

[31] D.S. Wishart, T. Jewison, A. Guo, et al., HMDB 3.0: The human metabolome database in 2013, Nucleic Acids Res 41 (2013) D801–D807.

[32] Z. Zhu, A.W. Schultz, J. Wang, et al., Liquid chromatography quadrupole time-of-flight mass spectrometry characterization of metabolites guided by the METLIN database, Nat. Protoc. 8 (2013) 451–460.

[33] F. De Chiara, K.L. Thomsen, A. Habtesion, et al., Ammonia scavenging prevents progression of fibrosis in experimental nonalcoholic fatty liver disease, Hepatology 71 (2020) 874–892.

[34] D. Montes-Cortes, I. Olivares-Corichi, J. Rosas-Barrientos, et al., Characterization of oxidative stress and ammonia according to the different grades of hepatic encephalopathy, Dig. Dis. 38 (2020) 240–250.

[35] C.N. Hsu, Y.L. Tain, Developmental programming and reprogramming of hypertension and kidney disease: Impact of tryptophan metabolism, Int. J. Mol. Sci. 21 (2020), 8705.

[36] X. Su, Y. Gao, R. Yang, Gut microbiota-derived tryptophan metabolites maintain gut and systemic homeostasis, Cells 11 (2022), 2296.

[37] C.A. Opitz, U.M. Litzenburger, F. Sahm, et al., An endogenous tumour-promoting ligand of the human aryl hydrocarbon receptor, Nature 478 (2011) 197–203.

[38] G.C. Prendergast, Cancer, Why tumours eat tryptophan, Nature 478 (2011) 192–194.

[39] A.B. Engin, B. Karahalil, A.E. Karakaya, et al., Exposure to helicobacter pylori and serum kynurenine to tryptophan ratio in patients with gastric cancer, Pteridines 21 (2010) 110–120.

[40] A.A.B. Badawy, Kynurenine pathway of tryptophan metabolism: Regulatory and functional aspects, Int. J. Tryptophan Res. 10 (2017), 1178646917691938.

[41] I. Sadok, K. Jędruchniewicz, K. Rawicz-Pruszyński, et al., UHPLC-ESI-MS/MS quantification of relevant substrates and metabolites of the kynurenine pathway present in serum and peritoneal fluid from gastric cancer patients—Method development and validation, Int. J. Mol. Sci. 22 (2021), 6972.

[42] J. Kuligowski, D. Sanjuan-Herráez, M.A. Vázquez-Sánchez, et al., Metabolomic analysis of gastric cancer progression within the *Correa*'s cascade using ultraperformance liquid chromatography–mass spectrometry, J. Proteome Res. 15 (2016) 2729–2738.

[43] B. Borowsky, N. Adham, K.A. Jones, et al., Trace amines: Identification of a family of mammalian G protein-coupled receptors, Proc. Natl. Acad. Sci. U. S. A. 98 (2001) 8966–8971.

[44] K. Gao, C. Mu, A. Farzi, et al., Tryptophan metabolism: A link between the gut microbiota and brain, Adv. Nutr. 11 (2020) 709–723.

[45] B.B. Williams, A.H. Van Benschoten, P. Cimermancic, et al., Discovery and characterization of gut microbiota decarboxylases that can produce the neurotransmitter tryptamine, Cell Host Microbe 16 (2014) 495–503.

[46] W. Liang, Y. Yang, H. Wang, et al., Gut microbiota shifts in patients with gastric cancer in perioperative period, Medicine (Baltimore) 98 (2019), e16626.

[47] Y.Y. Hsieh, S.Y. Tung, H.Y. Pan, et al., Increased abundance of *Clostridium* and *Fusobacterium* in gastric microbiota of patients with gastric cancer in Taiwan, Sci. Rep. 8 (2018) 158–168.

[48] C.W. Wu, C.W. Chi, E.C. Lin, et al., Serum arginase level in patients with gastric cancer, J. Clin. Gastroenterol. 18 (1994) 84–85.

[49] C.W. Wu, S.R. Wang, T.J. Chang, et al., Content of glucocorticoid receptor and arginase in gastric cancer and normal gastric mucosal tissues, Cancer 64 (1989) 2552–2556.

[50] P.C. Rodriguez, D.G. Quiceno, J. Zabaleta, et al., Arginase I production in the tumor microenvironment by mature myeloid cells inhibits T-cell receptor expression and antigen-specific T-cell responses, Cancer Res. 64 (2004) 5839–5849.

[51] F. Niu, Y. Yu, Z. Li, et al., Arginase: An emerging and promising therapeutic target for cancer treatment, Biomed. Pharmacother. 149 (2022), 112840.